Deformation effects and neutrinoless positron $\beta\beta$ decay of ^{96}Ru, ^{102}Pd, ^{106}Cd, ^{124}Xe, ^{130}Ba and ^{156}Dy isotopes within Majorona neutrino mass mechanism

P. K. Rath[1], R. Chandra[1,2], K. Chaturvedi[1,3], P. K. Raina[2] and J. G. Hirsch[4]
[1]*Department of Physics, University of Lucknow, Lucknow-226007, India*
[2]*Department of Physics and Meteorology, IIT, Kharagpur-721302, India*
[3]*Department of Physics, Bundelkhand University, Jhansi-284128, India*
[4]*Instituto de Ciencias Nucleares, Universidad Nacional Autónoma de México, A.P. 70-543, México 04510 D.F., México*
(Dated: October 8, 2009)

The $\left(\beta^+\beta^+\right)_{0\nu}$ and $\left(\varepsilon\beta^+\right)_{0\nu}$ modes of ^{96}Ru, ^{102}Pd, ^{106}Cd, ^{124}Xe, ^{130}Ba and ^{156}Dy isotopes are studied in the Projected Hartree-Fock-Bogoliubov framework for the $0^+ \to 0^+$ transition. The reliability of the intrinsic wave functions required to study these decay modes has been established in our earlier works by obtaining an overall agreement between the theoretically calculated spectroscopic properties, namely yrast spectra, reduced $B(E2{:}0^+ \to 2^+)$ transition probabilities, quadrupole moments $Q(2^+)$ and gyromagnetic factors $g(2^+)$ and the available experimental data in the parent and daugther even-even nuclei. In the present work, the required nuclear transition matrix elements are calculated in the Majorana neutrino mass mechanism using the same set of intrinsic wave functions as used to study the two neutrino positron double-β decay modes. Limits on effective light neutrino mass $\langle m_\nu \rangle$ and effective heavy neutrino mass $\langle M_N \rangle$ are extracted from the observed limits on half-lives $T_{1/2}^{0\nu}(0^+ \to 0^+)$ of $\left(\beta^+\beta^+\right)_{0\nu}$ and $\left(\varepsilon\beta^+\right)_{0\nu}$ modes. We also investigate the effect of quadrupolar correlations vis-a-vis deformation on NTMEs required to study the $\left(\beta^+\beta^+\right)_{0\nu}$ and $\left(\varepsilon\beta^+\right)_{0\nu}$ modes.

PACS numbers: 23.40.Bw, 23.40.Hc, 27.60.+j, 27.70.+q

I. INTRODUCTION

The sixteen rare, experimentally distinguishable, modes of nuclear $\beta\beta$ decay, namely the double-electron emission $(\beta^-\beta^-)$, double-positron emission $(\beta^+\beta^+)$, electron-positron conversion $(\varepsilon\beta^+)$ and double-electron capture $(\varepsilon\varepsilon)$ with the emission of two neutrinos, no neutrinos, single Majoron and double Majorons, are semileptonic weak transitions involving strangeness conserving charged currents. The $\beta^+\beta^+$, $\varepsilon\beta^+$ and $\varepsilon\varepsilon$ modes are energetically competing and we shall refer to them as $e^+\beta\beta$ decay. The experimental as well as theoretical study of nuclear $\beta^-\beta^-$ mode has been excellently reviewed over the past decades, which can be found in the recent review [1] and references there in. Also, the experimental and theoretical studies devoted to the $e^+\beta\beta$ decay have been reviewed over the past years [2, 3, 4, 5, 6, 7, 8, 9, 10, 11]. Owing to the confirmation of flavour oscillation of neutrinos at atmospheric, solar, reactor and accelerator neutrino sources, it has been established that neutrinos have mass. However, it is generally agreed that the observation of $(\beta\beta)_{0\nu}$ decay can clarify a number of issues regarding the nature of neutrinos, namely the origin of neutrino mass (Dirac vs. Majorana), the absolute scale on neutrino mass, the type of hierarchy and CP violation in the leptonic sector, etc. Further, the possible mechanisms for the occurrence of the lepton number violating $(\beta\beta)_{0\nu}$ decay are the exchange of light as well as heavy neutrinos and the right handed currents in the LRSM, the exchange of sleptons, neutralinos, squarks and gluinos in the R_p-violating MSSM, the exchange of leptoquarks, existence of heavy sterile neutrinos, compositeness and extradimensional scenarios. In nine Majoron models, namely IB, IC, IIB, IIC, IIF, ID, IE, IID and IIE [12], the single Majoron accompanied neutrinoless double beta $(\beta\beta\phi)_{0\nu}$ decay and double Majoron accompanied neutrinoless double beta $(\beta\beta\phi\phi)_{0\nu}$ decay occur in the former five and the latter four, respectively. The study of $(\beta\beta)_{0\nu}$ decay can provide stringent limits on the associated gauge theoretical parameters and its observation can only ascertain the role of various possible mechanisms in different gauge theoretical models.

In principle, the $\beta^-\beta^-$ decay and $e^+\beta\beta$ decay can provide us with the same but complementary information. The observation of $(e^+\beta\beta)_{2\nu}$ decay modes will be interesting from the nuclear structure point of view, as it is a challenging task to calculate the nuclear transition matrix elements (NTMEs) of these modes along with $(\beta^-\beta^-)_{2\nu}$ mode in the same theoretical framework. Further, the observation of $(e^+\beta\beta)_{0\nu}$ decay modes will be helpful in deciding issues like dominance of mass mechanism or right handed currents [13]. In an attempt to study the role of m_ν, λ and η mechanisms, Klapdor-Kleingrothaus *et al.* have analyzed the 71.7 kg.y data collected from 1990-2003 on enriched ^{76}Ge [14] and have shown that there is an apparent degeneracy in the parameters [15]. It has been also concluded that the analysis of a high sensitive $(\beta^-\beta^-)_{0\nu}$ experiment e.g. ^{76}Ge and a suitable high sensitive mixed mode decay e.g. ^{124}Xe is more advantageous [13].

In spite of the fact that the kinetic energy release in the $(\varepsilon\varepsilon)_{0\nu}$ mode is the largest, the experimental and theoretical study of this mode has not been attempted so far. The conservation of energy-momentum requires the emission of an additional particle in the $(\varepsilon\varepsilon)_{0\nu}$ mode. Further, the emission of one real photon is forbidden for the $0^+ \to 0^+$ transition if atomic electrons are absorbed from the K-shell. Therefore, one has to consider various

processes such as internal pair production, internal conversion, emission of two photons, L-capture etc. [6]. The decay rates of the above mentioned processes have to be calculated at least by the third order perturbation theory. Resultingly, there is a suppression factor of the order of 10^{-4} in comparison to the $(\varepsilon\beta^+)_{0\nu}$ mode. Hence, the experimental as well as theoretical study of $(e^+\beta\beta)_{0\nu}$ decay has been restricted to $(\beta^+\beta^+)_{0\nu}$ and $(\varepsilon\beta^+)_{0\nu}$ modes only. Arguably, Sujkowski and Wycech [16] have shown that there will be resonant enhancement of the $(\varepsilon\varepsilon)_{0\nu}$ mode if the nuclear levels in parent and daughter nuclei are almost degenerate i.e. $Q-(E_{2P}-E_{2S}) \sim 1\ keV$, where the energy difference is for atomic levels. Interestingly, Barabash *et al.* have reported that there might be a degeneracy between the ^{112}Sn ground state and an excited 0^+ state at 1870.9 keV in ^{112}Cd fulfilling the resonance enhancement condition for the $(\varepsilon\varepsilon)_{0\nu}$ mode [17]. It is expected that the study of this $(\varepsilon\varepsilon)_{0\nu}$ mode may be interesting in the near future.

The complex structure of nuclei in general, and of mass region $96 < A < 156$ in particular, is due to the subtle interplay of pairing and multipolar correlations present in the effective two-body interaction. The mass regions $A \sim 100$ and 150 offer nice examples of shape transitions at $N = 60$ and 90, respectively. The nuclei are soft vibrators for neutron number $N < 60$ and $N < 90$ and quasi-rotors for $N > 60$ and $N > 90$. Nuclei with neutron numbers $N = 60$ and 90 are transitional nuclei. The yrast spectra of Te and Xe isotopes, on the other hand, follow an approximate inverse parabolic type of systematics with minimum energy of 2^+ states occurring for ^{120}Te and ^{120}Xe isotopes, respectively. In this mass region $96 < A < 156$, the deformation parameters β_2 are in the range $(0.1409 \pm 0.0046) - (0.3378 \pm 0.0018)$ corresponding to ^{132}Xe and ^{156}Gd isotopes, respectively and hence, it is clear that deformation plays a crucial role in reproducing the properties of these nuclei. In nuclear $\beta\beta$ decay, the role of deformation degrees of freedom in addition to pairing correlation has been already stressed [18, 19]. Recently, the effects of pairing and quadrupolar correlations on the NTMEs of $(\beta^-\beta^-)_{0\nu}$ mode has been studied in the ISM [20, 21]. In the PHFB model, the role of deformation effects due to quadrupolar [22, 23, 24, 25] and multipolar correlations [26] has been also studied.

The shell model is the best choice for calculating the NTMEs as it attempts to solve the nuclear many-body problem as exactly as possible. However, the first explanation about the observed suppression of $M_{2\nu}$ was provided in the QRPA model by Vogel and Zirnbauer [27] and Civitarese *et al*. [28]. Further, the QRPA and its extensions have emerged as the most successful models in correlating single-β GT strengths and half-lives of $(\beta^-\beta^-)_{2\nu}$ mode. In spite of the spectacular success of the QRPA in the study of $\beta\beta$ decay, the necessity to include the deformation degrees of freedom in its formalism led to the development of the deformed QRPA model for studying $\beta\beta$ decay of spherical as well as deformed nuclei. The effect of deformation on the $(\beta^-\beta^-)_{2\nu}$ mode for the ground state transition ^{76}Ge $\rightarrow$ ^{76}Se was studied in the framework of deformed QRPA with separable GT residual interaction [29] and, very recently, employing realistic forces [30]. A deformed QRPA formalism to describe simultaneously the energy distributions of the single-β GT strength and the $(\beta^-\beta^-)_{2\nu}$ mode matrix elements for ^{48}Ca, ^{76}Ge, ^{82}Se, ^{96}Zr, ^{100}Mo, ^{116}Cd, ^{128,130}Te, ^{136}Xe and ^{150}Nd isotopes using deformed Woods-Saxon potential and deformed Skyrme Hartree-Fock mean field was developed [31]. Rodin and Faessler [32] have studied the $\beta^-\beta^-$ decay of ^{76}Ge, ^{100}Mo and ^{130}Te isotopes and it has been reported that the effect of continuum on the NTMEs of $(\beta^-\beta^-)_{2\nu}$ mode is negligible whereas the NTMEs of $(\beta^-\beta^-)_{0\nu}$ mode are regularly suppressed.

In the PHFB model, the interplay of pairing and deformation degrees of freedom are treated simultaneously and on equal footing. However, the structure of the intermediate odd Z-odd N nuclei, which provide information on the single-β decay rates and the distribution of GT strengths, can not be studied in the present version of the PHFB model. In spite of this limitation, the PHFB model, in conjunction with pairing plus quadrupole-quadrupole (PQQ) [33] interaction has been successfully applied to study the $0^+ \rightarrow 0^+$ transition of $(\beta^-\beta^-)_{2\nu}$ mode, where it was possible to describe the lowest excited states of the parent and daughter nuclei along with their electromagnetic transition strengths, as well as to reproduce their measured $\beta^-\beta^-$ decay rates [22, 24]. The main purpose of using the PQQ interaction is to study the interplay between sphericity and deformation. In this way, the PHFB formalism, employed in conjunction with the PQQ interaction, is a convenient choice to examine the explicit role of deformation on the NTMEs. The existence of an inverse correlation between the quadrupole deformation and the size of NTME $M_{2\nu}$ has been also confirmed [22, 23, 24]. In addition, it has been observed that the NTMEs for $\beta^-\beta^-$ decay are usually large in the absence of quadrupolar correlations. With the inclusion of the quadrupolar correlations, the NTMEs are almost constant for small admixture of the QQ interaction and suppressed substantially in realistic situation. It was also shown that the NTMEs of $\beta^-\beta^-$ decay have a well defined maximum when the deformation of parent and daughter nuclei are similar and they are suppressed for a difference in deformations in agreement with previous QRPA calculations [29]. The deformation effects are also of equal importance in the case of $(\beta^-\beta^-)_{2\nu}$ and $(\beta^-\beta^-)_{0\nu}$ modes [25, 26].

Moreover, the PHFB model along with the PQQ interaction in conjunction with the summation method has been successfully applied to study the $(e^+\beta\beta)_{2\nu}$ decay of ^{96}Ru, ^{102}Pd, ^{106,108}Cd, ^{124,126}Xe, ^{130,132}Ba [23, 24] and ^{156}Dy [34] isotopes for the $0^+ \rightarrow 0^+$ transition, not in isolation but together with other observed nuclear spectroscopic properties, namely yrast spectra, reduced $B(E2{:}0^+ \rightarrow 2^+)$ transition probabilities, quadrupole moments $Q(2^+)$ and gyromagnetic factors $g(2^+)$. This success of the PHFB model has prompted us to apply the

same to study the $0^+ \to 0^+$ transition of $(\beta^+\beta^+)_{0\nu}$ and $(\varepsilon\beta^+)_{0\nu}$ modes for the above mentioned nuclei. It has been observed that in general, there exists an anticorrelation between the magnitude of the quadrupolar deformation and the NTMEs $M_{2\nu}$ of $(e^+\beta\beta)_{2\nu}$ decay. In the case of $(e^+\beta\beta)_{2\nu}$ decay, we observed that the deformation plays an important role in the suppression of $M_{2\nu}$ by a factor of 2–13.6 approximately [23, 24, 34]. Therefore, we aim to study the variation of NTMEs of $(\beta^+\beta^+)_{0\nu}$ and $(\varepsilon\beta^+)_{0\nu}$ modes vis-a-vis the change in deformation by changing the strength of the QQ interaction.

The present paper is organized as follows. The theoretical formalism for calculating the half-lives of $(\beta^+\beta^+)_{0\nu}$ and $(\varepsilon\beta^+)_{0\nu}$ modes has been given by Doi *et al.* [6]. Hence, we briefly outline steps of the detailed derivations in Sec. II. In Sec. III, we present the results and discuss them vis-a-vis the existing calculations done in other nuclear models. In the study of $(\beta\beta)_{0\nu}$ decay, the practice is to either extract limits on various gauge theoretical parameters from the observed limits on half-lives of the $(\beta\beta)_{0\nu}$ decay or predict half-lives assuming certain value for the neutrino mass. Presently, the available experimental limits on half-lives of $(\beta^+\beta^+)_{0\nu}$ and $(\varepsilon\beta^+)_{0\nu}$ modes are not large enough to provide stringent limits on the effective gauge theoretical parameters $\langle m_\nu \rangle$ and $\langle M_N \rangle$. Therefore, we also predict half-lives $T^{0\nu}_{1/2}(0^+ \to 0^+)$ of $(\beta^+\beta^+)_{0\nu}$ and $(\varepsilon\beta^+)_{0\nu}$ modes for ^{96}Ru, ^{102}Pd, ^{106}Cd, ^{124}Xe, ^{130}Ba and ^{156}Dy isotopes, which will be helpful in the future experimental studies of $(e^+\beta\beta)_{0\nu}$ decay. In addition, we study the deformation effect on NTMEs of $(\beta^+\beta^+)_{0\nu}$ and $(\varepsilon\beta^+)_{0\nu}$ modes and show that the NTMEs have well defined maximum for similar deformations of parent and daughter nuclei and they are suppressed for a difference in deformations. Finally, the conclusions are given in Sec. IV.

II. THEORETICAL FORMALISM

In the Majorana neutrino mass mechanism, the effective charged current weak interaction Hamiltonian density H_W for β^+ decay due to W-boson exchange including hadronic currents can be written as

$$H_W = \frac{G}{\sqrt{2}} j_{L\mu} J_L^{\mu\dagger} + h.c.. \tag{1}$$

The left handed $V - A$ leptonic and hadronic currents for β^+ decay are given by

$$j_L^\mu = \overline{\nu_{eL}} \gamma^\mu (1 - \gamma_5) e, \tag{2}$$

$$J_L^{\mu\dagger} = g_v \overline{d} \gamma^\mu (1 - \gamma_5) u, \tag{3}$$

where $g_v = \cos\theta_c$ and θ_c is the Cabibbo-Kobayashi-Maskawa (CKM) mixing angle for the left and right handed d and s quarks. Further,

$$\nu_{eL} = \sum_i U_{ei} N_{iL}. \tag{4}$$

The Majorana neutrino field N_i has mass m_i and the mixing matrices U of left handed neutrinos are normalized i.e. $\sum_i |U_{ei}|^2 = 1$.

Usually, the decay rates for the $0^+ \to 0^+$ transition of $(\beta^+\beta^+)_{0\nu}$ and $(\varepsilon\beta^+)_{0\nu}$ modes are derived by making the following assumptions:

(i) The light and heavy neutrino species of mass $m_i < 10$ eV and $m_i > 1$ GeV, respectively are only considered.

(ii) The nonrelativistic impulse approximation is assumed for the hadronic currents.

(iii) The recoil current is neglected. However, it has been shown by Šimkovic *et al.* [35] and Vergados [36] that the consideration of pseudoscalar and weak magnetism terms of recoil current reduce the NTMEs up to 30%, which needs to be further investigated.

(iv) The $s_{1/2}$ waves describe the final leptonic states.

(v) The calculation of phase space factors is made easier by considering no finite de Broglie wave length correction.

(vi) The CP conservation is assumed. Consequently, the effective light neutrino mass $\langle m_\nu \rangle$ and effective heavy neutrino mass $\langle M_N \rangle$ are real.

With these approximations, the inverse half-lives $T^{0\nu}_{1/2}$ for the $0^+ \to 0^+$ transition of $(\beta^+\beta^+)_{0\nu}$ and $(\varepsilon\beta^+)_{0\nu}$ modes in 2n mechanism are given by [6]

$$\begin{aligned}\left[T^{0\nu}_{1/2}(\beta)\right]^{-1} &= \left(\frac{\langle m_\nu \rangle}{m_e}\right)^2 G_{01}(\beta)\left(M_{GT} - M_F\right)^2 + \left(\frac{m_p}{\langle M_N \rangle}\right)^2 G_{01}(\beta)\left(M_{GTh} - M_{Fh}\right)^2 \\ &\quad + \left(\frac{\langle m_\nu \rangle}{m_e}\right)\left(\frac{m_p}{\langle M_N \rangle}\right) G_{01}(\beta)\left(M_{GT} - M_F\right)\left(M_{GTh} - M_{Fh}\right),\end{aligned} \tag{5}$$

where β denotes the $(\beta^+\beta^+)_{0\nu} / (\varepsilon\beta^+)_{0\nu}$ mode and

$$\langle m_\nu \rangle = {\sum_i}' U_{ei}^2 m_i, \qquad m_i < 10\ eV, \tag{6}$$

$$\langle M_N \rangle^{-1} = {\sum_i}'' U_{ei}^2 m_i^{-1}, \qquad m_i > 1\ GeV. \tag{7}$$

In the closure approximation, NTMEs M_F, M_{GT}, M_{Fh}

and M_{GTh} are written as

$$M_F = \left(\frac{g_V}{g_A}\right)^2 \sum_{n,m} \left\langle 0_F^+ \left\| H(r)\tau_n^- \tau_m^- \right\| 0_I^+ \right\rangle, \tag{8}$$

$$M_{GT} = \sum_{n,m} \left\langle 0_F^+ \left\| \sigma_n \cdot \sigma_m H(r)\tau_n^- \tau_m^- \right\| 0_I^+ \right\rangle, \tag{9}$$

$$M_{Fh} = 4\pi \left(M_p m_e\right)^{-1} \left(\frac{g_V}{g_A}\right)^2 \sum_{n,m} \left\langle 0_F^+ \left\| \delta\left(\mathbf{r}\right) \tau_n^- \tau_m^- \right\| 0_I^+ \right\rangle, \tag{10}$$

$$M_{GTh} = 4\pi \left(M_p m_e\right)^{-1} \sum_{n,m} \left\langle 0_F^+ \left\| \sigma_n \cdot \sigma_m \delta\left(\mathbf{r}\right) \tau_n^- \tau_m^- \right\| 0_I^+ \right\rangle. \tag{11}$$

The neutrino potential $H(r)$ arising due to the exchange of light neutrino is defined as

$$H\left(r\right) = \frac{4\pi R}{\left(2\pi\right)^3} \int d^3q \frac{\exp\left(i\mathbf{q}\cdot\mathbf{r}\right)}{\omega\left(\omega + \overline{A}\right)}, \tag{12}$$

with

$$\overline{A} = \langle E_N \rangle - \frac{1}{2}\left(E_I + E_F\right). \tag{13}$$

In addition, the inclusion of effects due to finite size of nucleons (FNS) and short range correlations (SRC) is required. The FNS is usually taken into account by a dipole type of form factor making the replacement

$$g_V \rightarrow g_V \left(\frac{\Lambda^2}{\Lambda^2 + k^2}\right)^2 \quad \text{and} \quad g_A \rightarrow g_A \left(\frac{\Lambda^2}{\Lambda^2 + k^2}\right)^2 \tag{14}$$

with $\Lambda = 850$ MeV. In the PHFB model, the configuration mixing takes care of the long range correlations. The effect of short range correlations (SRC), which arise mainly from the repulsive nucleon-nucleon potential due to the exchange of ρ and ω mesons, is usually absent. To study the $(\beta^-\beta^-)_{0\nu}$ mode, the SRC has been incorporated by Hirsch *et al.* through the exchange of ω-meson [37], Kortelainen *et al.* [38] as well as Šimkovic *et al.* [39] by using the unitary correlation operator method (UCOM) and Šimkovic *et al.* [40] by self-consistent CCM. This SRC effect can also be incorporated through phenomenological Jastrow type of correlation using Miller and Spencer parametrization by the prescription

$$\left\langle j_1^\pi j_2^\pi J \left| O \right| j_1^\nu j_2^\nu J' \right\rangle \rightarrow \left\langle j_1^\pi j_2^\pi J \left| fOf \right| j_1^\nu j_2^\nu J' \right\rangle, \tag{15}$$

where

$$f(r) = 1 - e^{-ar^2}(1 - br^2) \tag{16}$$

with $a = 1.1$ fm^{-2} and $b = 0.68$ fm^{-2} [41]. It has been shown by Wu and co-workers [42] that for the $(\beta^-\beta^-)_{0\nu}$ mode of ^{48}Ca, the phenomenologically determined $f(r)$ has strong two nucleon correlations in comparison to the effective transition operator $\widehat{f}O\widehat{f}$ derived using Reid and Paris potentials.

In the PHFB model, the calculation of the NTMEs M_α ($\alpha = F,\ GT,\ Fh$ and GTh) of the $(\beta^+\beta^+)_{0\nu}$ and $(\varepsilon\beta^+)_{0\nu}$ modes is carried out as follows. The two basic ingredients of the PHFB model are the existence of an independent quasiparticle mean field solution and the projection technique. To start with, amplitudes (u_{im}, v_{im}) and expansion coefficients $C_{ij,m}$ required to specify the axially symmetric HFB intrinsic state $|\Phi_0\rangle$ with $K = 0$ are obtained by carrying out the HFB calculation through the minimization of the expectation value of the effective Hamiltonian. Subsequently, states with good angular momentum $\mathbf{J}$ are obtained from $|\Phi_0\rangle$ using the standard projection technique [43] given by

$$|\Psi_{00}^J\rangle = \frac{(2J+1)}{8\pi^2} \int D_{00}^J(\Omega) R(\Omega) |\Phi_0\rangle d\Omega, \tag{17}$$

where $R(\Omega)$ and $D_{00}^J(\Omega)$ are the rotation operator and the rotation matrix, respectively. Further,

$$|\Phi_0\rangle = \prod_{im} (u_{im} + v_{im} b_{im}^\dagger b_{i\bar{m}}^\dagger)|0\rangle \tag{18}$$

with the creation operators $b_{im}^\dagger$ and $b_{i\bar{m}}^\dagger$ defined as

$$b_{im}^\dagger = \sum_\alpha C_{i\alpha,m} a_{\alpha m}^\dagger \text{ and } b_{i\bar{m}}^\dagger = \sum_\alpha (-1)^{l+j-m} C_{i\alpha,m} a_{\alpha,-m}^\dagger. \tag{19}$$

Finally, the NTMEs M_α of the $(\beta^+\beta^+)_{0\nu}$ and $(\varepsilon\beta^+)_{0\nu}$ modes are given by

$$\begin{aligned}
M_\alpha &= \langle \Psi_{00}^{J_f=0} || O_\alpha \tau^- \tau^- || \Psi_{00}^{J_i=0} \rangle \\
&= [n_{Z,N}^{J_i=0} n_{Z-2,N+2}^{J_f=0}]^{-1/2} \\
&\quad \times \int_0^\pi n_{(Z,N),(Z-2,N+2)}(\theta) \sum_{\alpha\beta\gamma\delta} \left\langle \alpha\beta \left| O_\alpha \tau^- \tau^- \right| \gamma\delta \right\rangle \\
&\quad \times \sum_{\varepsilon\eta} \frac{(f_{Z-2,N+2}^{(\nu)*})_{\varepsilon\beta}}{\left[1 + F_{Z,N}^{(\nu)}(\theta) f_{Z-2,N+2}^{(\nu)*}\right]_{\varepsilon\alpha}} \\
&\quad \times \frac{(F_{Z,N}^{(\pi)*})_{\eta\delta}}{\left[1 + F_{Z,N}^{(\pi)}(\theta) f_{Z-2,N+2}^{(\pi)*}\right]_{\gamma\eta}} \sin\theta d\theta, \qquad (20)
\end{aligned}$$

where

$$\begin{aligned}
n^J &= \int_0^\pi \{\det[1 + F^{(\pi)}(\theta) f^{(\pi)\dagger}]\}^{1/2} \\
&\quad \times \{\det[1 + F^{(\nu)}(\theta) f^{(\nu)\dagger}]\}^{1/2} d_{00}^J(\theta) \sin(\theta) d\theta
\end{aligned} \qquad (21)$$

and

$$\begin{aligned}
n_{(Z,N),(Z-2,N+2)}(\theta) &= \{\det[1 + F_{Z,N}^{(\pi)}(\theta) f_{Z-2,N+2}^{(\pi)\dagger}]\}^{1/2} \\
&\quad \times \{\det[1 + F_{Z,N}^{(\nu)}(\theta) f_{Z-2,N+2}^{(\nu)\dagger}]\}^{1/2}.
\end{aligned} \qquad (22)$$

The $\pi(\nu)$ represents the proton (neutron) of nuclei involved in the $(\beta^+\beta^+)_{0\nu} / (\varepsilon\beta^+)_{0\nu}$ mode. The matrices $f_{Z,N}$ and $F_{Z,N}(\theta)$ are given by

$$[f_{Z,N}]_{\alpha\beta} = \sum_i C_{ij_\alpha,m_\alpha} C_{ij_\beta,m_\beta} \left(v_{im_\alpha}/u_{im_\alpha}\right) \delta_{m_\alpha,-m_\beta} \qquad (23)$$

and

$$[F_{Z,N}(\theta)]_{\alpha\beta} = \sum_{m'_\alpha m'_\beta} d^{j_\alpha}_{m_\alpha,m'_\alpha}(\theta) d^{j_\beta}_{m_\beta,m'_\beta}(\theta) f_{j_\alpha m'_\alpha, j_\beta m'_\beta}. \qquad (24)$$

To calculate NTMEs M_α of the $(\beta^+\beta^+)_{0\nu}$ and $(\varepsilon\beta^+)_{0\nu}$ modes, the matrices $[f_{Z,N}]_{\alpha\beta}$ and $[F_{Z,N}(\theta)]_{\alpha\beta}$ are evaluated using expressions given by Eqs. (23) and (24), respectively. The required NTMEs M_α are obtained using Eq. (20) with 20 gaussian quadrature points in the range (0, π).

III. RESULTS AND DISCUSSIONS

The model space, single particle energies (SPE's) and parameters of the effective two-body interaction are the same as our earlier calculations on $(e^+\beta\beta)_{2\nu}$ decay of ^{96}Ru, ^{102}Pd, ^{106,108}Cd [23], ^{124,126}Xe, ^{130,132}Ba [24] and ^{156}Dy [34] isotopes for the $0^+ \to 0^+$ transition. We briefly present a discussion about them for the sake of completeness as well as present convenience. The doubly even ^{76}Sr ($N = Z = 38$) and ^{100}Sn ($N = Z = 50$) nuclei were treated as inert cores for the nuclei in the mass region $A = 96 - 108$ and $A = 124 - 156$, respectively. The change of model space was forced upon because the number of neutrons increase to about 40 for nuclei occurring in the mass region $A = 130$ and with the increase in neutron number, the yrast energy spectra was compressed due to increase in the attractive part of effective two-body interaction. In Table I, we have given the single particle orbits, which span the valence space and corresponding SPEs. In the model space with ^{76}Sr core, the $1p_{1/2}$ orbit was included to examine the role of the $Z = 40$ proton core vis-a-vis the onset of deformation in the highly neutron rich isotopes. For ^{156}Dy and ^{156}Gd isotopes, the SPE's used for $0h_{11/2}$, $1f_{7/2}$ and $0h_{9/2}$ orbits were 4.6 MeV, 11.0 MeV and 11.6 MeV, respectively.

TABLE I: Single particle orbits of the model space and SPEs for protons and neutrons.

$A = 96 - 108$		$A = 124 - 156$	
Orbits	ε (MeV)	Orbits	ε (MeV)
$1p_{1/2}$	-0.8	$2s_{1/2}$	1.4
$2s_{1/2}$	6.4	$1d_{3/2}$	2.0
$1d_{3/2}$	7.9	$1d_{5/2}$	0.0
$1d_{5/2}$	5.4	$1f_{7/2}$	12.0
$0g_{7/2}$	8.4	$0g_{7/2}$	4.0
$0g_{9/2}$	0.0	$0h_{9/2}$	12.5
$0h_{11/2}$	8.6	$0h_{11/2}$	6.5

The HFB wave functions were generated by using an effective Hamiltonian with PQQ type of effective two-body interaction [33] given by

$$H = H_{sp} + V(P) + \zeta_{qq} V(QQ), \qquad (25)$$

where H_{sp}, $V(P)$ and $V(QQ)$ represent the single particle Hamiltonian, the pairing and quadrupole-quadrupole part of the effective two-body interaction, respectively. The arbitrary parameter ζ_{qq} was introduced to study the role of deformation by varying the strength of QQ interaction and the final results were obtained by using $\zeta_{qq} = 1$. Following Heestand *et al.* [44], who have used $G_p = 30/A$ MeV and $G_n = 20/A$ MeV to explain the experimental $g(2^+)$ data of some even-even Ge, Se, Mo, Ru, Pd, Cd and Te isotopes in Greiner's collective model [45], we used the same strengths for $A = 96 - 108$ nuclei. In the case of $A = 124 - 132$ isotopes, the strengths of the pairing interaction were fixed as $G_p = G_n = 35/A$ MeV. However, we used $G_p = G_n = 30/A$ MeV for ^{156}Dy and ^{156}Gd isotopes.

The parameters of the QQ interaction were fixed as follows. The strengths of the like particle components χ_{pp} and χ_{nn} were taken as 0.0105 MeV b^{-4}, where b is oscillator parameter. The strength of proton-neutron (pn)

component χ_{pn} was varied so as to obtain the spectra of considered nuclei $A = 96 - 156$ in optimum agreement with the experimental data. The theoretical spectra was taken to be the optimum one if the excitation energy of the 2^+ state E_{2^+} was reproduced as closely as possible to the experimental value. All the parameters were kept fixed throughout the subsequent calculations. The reliability of HFB wave functions was tested by obtaining an over all agreement between theoretically calculated results for the yrast spectra, reduced $B(E2{:}0^+ \to 2^+)$ transition probabilities, static quadrupole moments $Q(2^+)$ as well as g-factors $g(2^+)$ of the above mentioned nuclei and the available experimental data. The same PHFB wave functions were employed to calculate NTMEs $M_{2\nu}$ and half-lives $T_{1/2}^{2\nu}(0^+ \to 0^+)$ of $(e^+\beta\beta)_{2\nu}$ decay for ^{96}Ru, ^{102}Pd, ^{106,108}Cd [23], ^{124,126}Xe, ^{130,132}Ba [24] and ^{156}Dy [34] isotopes. It was also shown that the proton-neutron part of the PQQ interaction, which is responsible for triggering deformation in the intrinsic ground state, plays an important role in the suppression of $M_{2\nu}$.

A. Results of $(\beta^+\beta^+)_{0\nu}$ and $(\varepsilon\beta^+)_{0\nu}$ modes

The phase space factors G_{01} of $(\beta^+\beta^+)_{0\nu}$ and $(\varepsilon\beta^+)_{0\nu}$ modes have been evaluated by Doi *et al.* with $g_A = 1.261$ [6]. We use the phase space factors after reevaluating them for $g_A = 1.254$. The phase space factors of $\beta^+\beta^+$ $(\varepsilon\beta^+)$ modes (in yr^{-1}) used in the present calculation are 2.243×10^{-18} (2.664×10^{-17}), 2.532×10^{-18} (3.635×10^{-17}), 3.048×10^{-18} (5.654×10^{-17}) and 5.114×10^{-19} (4.901×10^{-17}) for ^{96}Ru,^{106}Cd, ^{124}Xe and ^{130}Ba nuclei, respectively [6]. For ^{102}Pd and ^{156}Dy nuclei, we calculate G_{01} following the notations of Doi *et al.* [6] in the approximation $C_1 = 1.0$, $C_2 = 0.0$, $C_3 = 0.0$ and $R_{1,1}(\varepsilon) = R_{+1}(\varepsilon) + R_{-1}(\varepsilon) = 1.0$. The calculated G_{01} of the $\varepsilon\beta^+$ mode for ^{102}Pd and ^{156}Dy isotopes are 6.0×10^{-19} yr^{-1} and 3.250×10^{-17} yr^{-1}, respectively.

In Table II, the NTMEs M_F, M_{GT}, M_{Fh} and M_{GTh} required to study the $(\beta^+\beta^+)_{0\nu}$ and $(\varepsilon\beta^+)_{0\nu}$ modes of ^{96}Ru, ^{102}Pd, ^{106}Cd, ^{124}Xe, ^{130}Ba and ^{156}Dy nuclei are compiled. Following Haxton's prescription [46], the average energy denominator is taken as $\overline{A} = 1.2A^{1/2}$ MeV. We calculate the four NTMEs in the approximation of point nucleons, point nucleons plus Jastrow type of SRC with Miller and Spencer parametrization [41], finite size of nucleons with dipole form factor and finite size plus SRC. In the case of point nucleons, the NTMEs M_F and M_{GT} are calculated for $\overline{A}$ and $\overline{A}/2$ in the energy denominator. It is observed that the NTMEs M_F and M_{GT} change by 7.8–9.8% for $\overline{A}/2$ in comparison to $\overline{A}$ in the energy denominator. Therefore, the dependence of NTMEs on average excitation energy $\overline{A}$ is small and the closure approximation is quite good in the case of $(\beta^+\beta^+)_{0\nu}$ and $(\varepsilon\beta^+)_{0\nu}$ modes as expected. In the approximation of light neutrinos, the NTMEs M_F and M_{GT} are reduced by 17.8–21.4% and 12.2–14.2% for point nucleon plus SRC, and finite size of nucleons respectively. Finally, the NTMEs change by 21.7–25.8% with finite size plus SRC. In the case of heavy neutrinos, the M_{Fh} and M_{GTh} get reduced by 33.9–38.0% and 65.0–68.5% with the inclusion of finite size and finite size plus SRC.

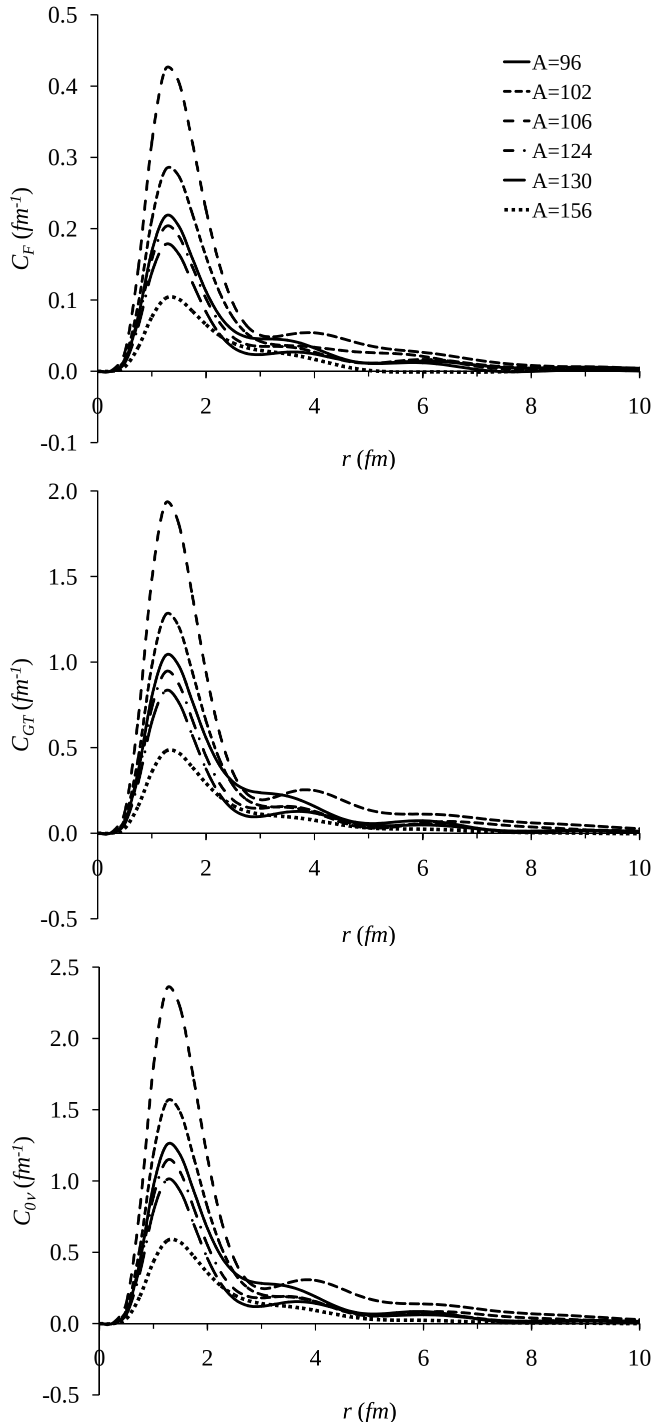

FIG. 1: Radial dependence of $C_F(r)$, $C_{GT}(r)$ and $C_{0\nu}(r)$ with FNS and SRC effects for the $(\beta^+\beta^+)_{0\nu}$ and $(\varepsilon\beta^+)_{0\nu}$ decay modes of ^{96}Ru, ^{102}Pd, ^{106}Cd, ^{124}Xe, ^{130}Ba and ^{156}Dy isotopes.

TABLE II: Calculated NTMEs for the $0^+ \rightarrow 0^+$ transition of $\left(\beta^+\beta^+\right)_{0\nu}$ and $\left(\varepsilon\beta^+\right)_{0\nu}$ modes in the mass mechanism.

Nuclei	NTMEs	Point $\overline{A}$	Point $\overline{A}/2$	Point+SRC	Extened	Extended+SRC
^{96}Ru	M_F	0.4983	0.5372	0.3969	0.4309	0.3757
	M_{GT}	-2.4780	-2.6826	-2.0000	-2.1591	-1.8992
	M_{Fh}	35.8917		0	22.4117	11.4829
	M_{GTh}	-169.321		0	-106.353	-54.7130
^{102}Pd	M_F	0.6464	0.6995	0.5233	0.5632	0.4965
	M_{GT}	-2.7663	-2.9861	-2.1863	-2.3785	-2.0631
	M_{Fh}	43.3140		0	28.1494	14.7508
	M_{GTh}	-204.336		0	-129.721	-67.0114
^{106}Cd	M_F	0.9583	1.0394	0.7704	0.8319	0.7299
	M_{GT}	-4.3495	-4.7284	-3.4635	-3.7594	-3.2769
	M_{Fh}	66.1196		0	42.5989	22.1888
	M_{GTh}	-311.922		0	-197.061	-101.408
^{124}Xe	M_F	0.4865	0.5333	0.3915	0.4233	0.3717
	M_{GT}	-2.1387	-2.3299	-1.6905	-1.8416	-1.5978
	M_{Fh}	33.7569		0	21.1455	10.8449
	M_{GTh}	-159.250		0	-98.9817	-50.4944
^{130}Ba	M_F	0.4183	0.4593	0.3338	0.3623	0.3163
	M_{GT}	-1.8626	-2.0325	-1.4633	-1.5986	-1.3812
	M_{Fh}	30.0461		0	18.7025	9.5438
	M_{GTh}	-141.744		0	-87.8418	-44.6828
^{156}Dy	M_F	0.2461	0.2698	0.2022	0.2160	0.1926
	M_{GT}	-1.1281	-1.2319	-0.9208	-0.9867	-0.8754
	M_{Fh}	15.7014		0	10.3729	5.4997
	M_{GTh}	-74.0722		0	-48.6696	-25.6980

The radial dependence of $C_{0\nu}(r)$ defined by

$$M_{0\nu} = \int_0^\infty C_{0\nu}(r)\, dr \tag{26}$$

has been studied in the QRPA by Šimkovic *et al.* [39] and ISM by Menéndez *et al.* [47]. In both QRPA and ISM calculations, it has been established that the contributions of decaying pairs coupled to $J = 0$ and $J > 0$ almost cancel beyond $r \approx 3$ fm and the magnitude of $C_{0\nu}(r)$ for all nuclei undergoing $(\beta^-\beta^-)_{0\nu}$ decay are the maximum about the internucleon distance $r \approx 1$ fm. In Fig. 1, we plot the radial dependence of the total matrix elements $C_{0\nu}(r)$ as well as their Fermi and Gamow-Teller components due to the exchange of light neutrinos. It is noticed that the maximum value of $C_F(r)$, $C_{GT}(r)$ and $C_{0\nu}(r)$ is at $r = 1.25$ fm in agreement with the works done by Šimkovic *et al.* [39] and Menéndez *et al.* [47].

In Table III, we tabulate the extracted limits on the effective light neutrino mass $< m_\nu >$ as well as heavy neutrino mass $< M_N >$ using presently available experimentally observed limits on half-lives of $(\beta^+\beta^+)_{0\nu}$ and $(\varepsilon\beta^+)_{0\nu}$ modes. It is observed that limits on $< m_\nu >$ and $< M_N >$ are not so much stringent as in the case of $(\beta^-\beta^-)_{0\nu}$ mode. Further, better limits are obtained in the case of $(\varepsilon\beta^+)_{0\nu}$ mode even for equal limits on half-lives of $(\beta^+\beta^+)_{0\nu}$ and $(\varepsilon\beta^+)_{0\nu}$ modes. In the case of $(\varepsilon\beta^+)_{0\nu}$ mode, the best limits obtained for ^{130}Ba nuclei are $< m_\nu >< 6.8 \times 10^2$ eV and $< M_N >> 2.25 \times 10^4$ GeV.

In Table IV, we compile available theoretical results in other nuclear models along with ours. To the best of our knowledge, no theoretical result and experimental half-life limit is available for ^{102}Pd and ^{156}Dy isotopes. Staudt *et al.* [52] have reported only NTMEs $|M_{0\nu}| = |M_{GT} - M_F|$ in the mass mechanism. In the QRPA calculations of Hirsch *et al.* [13] and Staudt *et al.* [52], the former used two major oscillator shells, where as the latter used a model space consisting of $3\hbar\omega + 4\hbar\omega + 0h_{9/2} + 0h_{11/2}$ orbits. The used SPEs are identical. Both the calculation use a realistic effective two body interaction using Paris potential. The NTMEs $|M_{0\nu}|$ are almost identical in both the QRPA calculations but for ^{124}Xe, where a difference by a factor of 1.8 approximately is noticed. In the SQRPA model, Stoica *et al.* [53] have studied $(\beta^+\beta^+)_{0\nu}$ and $(\varepsilon\beta^+)_{0\nu}$ modes of ^{106}Cd isotope

TABLE III: Upper and lower bounds on light and heavy neutrino effective masses $< m_\nu >$ and $< M_N >$, respectively, for the $\left(\beta^+\beta^+\right)_{0\nu}$ and $\left(\varepsilon\beta^+\right)_{0\nu}$ modes of ^{96}Ru, ^{106}Cd, ^{124}Xe and ^{130}Ba isotopes.

Nuclei	$T^{0\nu}_{1/2}$(yr)		Ref.	$< m_\nu > (eV)$		$< M_N > (GeV)$	
	$\beta^+\beta^+$	$\varepsilon\beta^+$		$\beta^+\beta^+$	$\varepsilon\beta^+$	$\beta^+\beta^+$	$\varepsilon\beta^+$
^{96}Ru	$> 3.1 \times 10^{16}$	$> 6.7 \times 10^{16}$	[48]	8.52×10^5	1.68×10^5	16.38	82.98
^{106}Cd	$> 1.4 \times 10^{19}$	$> 7.0 \times 10^{19}$	[49]	2.14×10^4	2.53×10^3	6.90×10^2	5.85×10^3
^{124}Xe	$> 4.2 \times 10^{17}$	$> 1.2 \times 10^{18}$	[50]	2.29×10^5	3.15×10^4	65.12	4.74×10^2
^{130}Ba	$> 4.0 \times 10^{21}$	$> 4.0 \times 10^{21}$	[51]	6.66×10^3	6.80×10^2	2.30×10^3	2.25×10^4

TABLE IV: Predicted half-lives $T^{0\nu}_{1/2} < m_\nu >^2$ of $\left(\beta^+\beta^+\right)_{0\nu}$ and $\left(\varepsilon\beta^+\right)_{0\nu}$ modes due to the exchange of light neutrino and extracted limits on effective heavy neutrino mass $\langle M_N \rangle$ from the same predicted half-lives for $< m_\nu >= 1$ eV. The † and ‡ denote WS and AWS basis respectively in reference [55].

Nuclei	Model	Ref.	M_F	M_{GT}	$\lvert M_{0\nu}\rvert$	$T^{0\nu}_{1/2} < m_\nu >^2$ (yr eV^2)		M_{Fh}	M_{GTh}	$\lvert M_{0N}\rvert$	$< M_N >$ (GeV)
						$\beta^+\beta^+$	$\varepsilon\beta^+$				
^{96} Ru	PHFB		0.376	-1.899	2.275	2.249×10^{28}	1.894×10^{27}	11.483	-54.713	66.196	1.40×10^7
	MCM	[54]	-0.705	1.678	2.383	2.050×10^{28}	1.726×10^{27}				
	QRPA	[13]	-0.98	2.62	3.60	8.981×10^{27}	7.563×10^{26}				
	QRPA	[52]			4.228	6.511×10^{27}	5.483×10^{26}				
^{102} Pd			0.497	-2.063	2.560		6.643×10^{28}	14.751	-67.011	81.762	1.53×10^7
^{106} Cd	PHFB		0.730	-3.277	4.007	6.424×10^{27}	4.474×10^{26}	22.189	-101.408	123.597	1.48×10^7
	MCM	[54]	-1.191	2.203	3.394	8.953×10^{27}	6.236×10^{26}				
	SQRPA(l)	[53]	-2.12	5.73	7.85	1.674×10^{27}	1.166×10^{26}				
	SQRPA(s)	[53]	-2.18	5.99	8.17	1.545×10^{27}	1.076×10^{26}				
	QRPA	[13]	-1.22	3.34	4.56	4.960×10^{27}	3.455×10^{26}				
	QRPA	[52]			4.778	4.517×10^{27}	3.146×10^{26}				
^{124} Xe	PHFB		0.372	-1.598	1.970	2.208×10^{28}	1.191×10^{27}	10.845	-50.494	61.339	1.49×10^7
	MCM	[54]	-2.572	5.729	8.301	1.243×10^{27}	6.703×10^{25}				
	QRPA†	[55]	-2.236	5.128	7.364	1.580×10^{27}	8.517×10^{25}				
	QRPA‡	[55]	-2.574	5.733	8.307	1.241×10^{27}	6.693×10^{25}				
	QRPA	[13]	-1.35	3.92	5.27	3.084×10^{27}	1.663×10^{26}				
	QRPA	[52]			2.975	9.678×10^{27}	5.218×10^{26}				
^{130}Ba	PHFB		0.316	-1.381	1.697	1.772×10^{29}	1.849×10^{27}	9.544	-44.683	54.227	1.53×10^7
	MCM	[54]	-1.748	3.382	5.130	1.940×10^{28}	2.025×10^{26}				
	QRPA	[13]	-1.50	4.02	5.52	1.676×10^{28}	1.749×10^{26}				
	QRPA	[52]			5.579	1.641×10^{28}	1.712×10^{26}				
^{156}Dy	PHFB		0.193	-0.875	1.068		7.044×10^{27}	5.500	-25.698	31.198	1.40×10^7

using two model spaces, namely small basis (oscillator shells of $3\hbar\omega - 5\hbar\omega + i_{13/2}$ orbits) and a large basis (oscillator shells of $2\hbar\omega - 5\hbar\omega + i_{13/2}$ orbits) with two-body effective interactions derived from the Bonn-A potential. The NTMEs calculated in the SQRPA [53] do not depend much on the model space and differ by a factor of 1.8 approximately from those of Hirsch *et al.* [13]. In the MCM, Suhonen *et al.* [54] have studied the $(\beta^+\beta^+)_{0\nu}$ and $(\varepsilon\beta^+)_{0\nu}$ modes of ^{96}Ru, ^{106}Cd, ^{124}Xe and ^{130}Ba nuclei. It is worth mentioning that besides the model space, SPEs and effective two-body interaction, different values of g_A, specifically $g_A = 1.254$ [13, 52, 53] and 1.0 [54, 55], are also used in these calulations.

The calculated NTMEs $|M_{0\nu}|$ in the PHFB model for the ^{96}Ru and ^{106}Cd isotopes are very close to those obtanied in the MCM, and in the later case also to the QRPA results. For ^{124}Xe and ^{130}Ba isotopes, the NTMEs are smaller than those in other models and this is reflected in half-lives which are up to one order of magnitude longer. As the extracted limits on the effective neutrino masses $< m_\nu >$ and $< M_N >$ are not stringent enough, it is more meaningful to calculate half-lives of $(\beta^+\beta^+)_{0\nu}$ and $(\varepsilon\beta^+)_{0\nu}$ modes, which will be useful for the design of future experimental set ups. Hence,

we calculate half-lives of $(\beta^+\beta^+)_{0\nu}$ and $(\varepsilon\beta^+)_{0\nu}$ modes for $< m_\nu >= 1\ eV$ and extract corresponding limits on heavy neutrino mass $< M_N >$, which are given in the same Table IV.

In the mass mechanisms, there are two noteworthy observations. The equality in NTMEs of $(\beta^+\beta^+)_{0\nu}$ and $(\varepsilon\beta^+)_{0\nu}$ modes implies that

$$\frac{T_{1/2}^{0\nu}\left(\beta^+\beta^+\right)}{T_{1/2}^{0\nu}\left(\varepsilon\beta^+\right)} = \frac{G_{01}\left(\varepsilon\beta^+\right)}{G_{01}\left(\beta^+\beta^+\right)}. \tag{27}$$

Therefore, the experimental observation of $(\varepsilon\beta^+)_{0\nu}$ mode will provide the half-life $T_{1/2}^{0\nu}\left(\beta^+\beta^+\right)$ of $(\beta^+\beta^+)_{0\nu}$ mode as the phase space factors are exactly calculable. Further, it is noticed that the ratios of $|M_{0\nu}|$ and $|M_{0N}|$ given in Table II are almost constant for different nuclei and $|M_{0N}|\,/\,|M_{0\nu}| \approx 29-32$ approximately. Similar behaviour of the ratios $|M_{0N}|\,/\,|M_{0\nu}| \approx 28-30$ is also observed for the NTMEs of $(\beta^-\beta^-)_{0\nu}$ mode [25]. This implies that in the mass mechanism, the half-lives for different nuclei due to exchange of light and heavy neutrinos are also in constant ratio

$$\frac{T_{1/2}^{0\nu}(m_\nu)}{T_{1/2}^{0\nu}(M_N)} \propto \frac{|M_{0N}|^2}{|M_{0\nu}|^2}. \tag{28}$$

It will be interesting to verify whether the observed constancy of $|M_{0N}|\,/\,|M_{0\nu}|$ in different nuclei is a generic feature or artifact of the present calculation.

B. Quadrupolar correlations and deformation effects

As already mentioned, the quadrupolar correlations are mainly responsible for the deformation of nuclei. To understand the role of deformation on NTMEs M_α ($\alpha = F, GT, Fh, GTh$) of $(\beta^+\beta^+)_{0\nu}$ and $(\varepsilon\beta^+)_{0\nu}$ modes, we investigate the variation of the latter by changing the strength of the QQ interaction ζ_{qq} for the case in which NTMEs are calculated with finite size and short range correlations. It is observed that in general, there is an inverse correlation between the magnitudes of NTMEs and quadrupole moments $Q(2^+)$ as well as deformation parameters β_2. Further, the effect of deformation on M_α is quantified by defining a quantity D_α as the ratio of M_α at zero deformation ($\zeta_{qq} = 0$) and full deformation ($\zeta_{qq} = 1$). The D_α is given by

$$D_\alpha = \frac{M_\alpha(\zeta_{qq} = 0)}{M_\alpha(\zeta_{qq} = 1)}. \tag{29}$$

The tabulated values of D_α in Table V for ^{96}Ru, ^{102}Pd, ^{106}Cd, ^{124}Xe, ^{130}Ba and ^{156}Dy nuclei suggest that the NTMEs M_α are suppressed by factor of 1.7–10.7 in the mass range $A = 96-156$ due to deformation effects. We also give the same deformation ratio $D_{2\nu}$ for comparison in the last row of the same table, which also change by almost same amount due to the deformation effects. Hence, it is clear that the deformation effects are important for $(\beta^+\beta^+)_{0\nu}$ and $(\varepsilon\beta^+)_{0\nu}$ modes as well as $(e^+\beta\beta)_{2\nu}$ decay so far as the nuclear structure aspect of $e^+\beta\beta$ decay is concerned.

In the left and right panels of Fig. 2 and 3, we present the variation of NTMEs $|M_{0\nu}|$ and $|M_{0N}|$ due to the light and heavy neutrino exchange, respectively, with respect to $\Delta\beta_2 = \beta_2(parent) -\ \beta_2(daughter)$ for the above mentioned $e^+\beta\beta$ emitters. The theoretically calculated deformation parameters β_2 for parent and daughter nuclei have been given in Refs. [23, 24] and we present them in Table VI for convenience. It can be noticed that the variation in $|M_{0\nu}|$ with changing $\Delta\beta_2$ is similar as that of $|M_{0N}|$. Moreover, it can be observed in Fig. 2 and 3 that the NTMEs remain constant even when one of the nuclei is spherical or slightly deformed. With further increase in deformation, the NTMEs in general become the maximum for $\Delta\beta_2 = 0$ and then decrease with increase in the difference between the deformation parameters. To summarize, the independent deformations of initial and final nuclei are important parameters to describe the NTMEs $M_{0\nu}$ and M_{0N} of $(\beta^+\beta^+)_{0\nu}$ and $(\varepsilon\beta^+)_{0\nu}$ modes.

TABLE V: Ratios D_α for ^{96}Ru, ^{102}Pd, ^{106}Cd, ^{124}Xe, ^{130}Ba and ^{156}Dy isotopes.

Ratios	^{96}Ru	^{102}Pd	^{106}Cd	^{124}Xe	^{130}Ba	^{156}Dy
D_F	2.92	2.52	1.91	3.83	4.68	10.42
D_{GT}	2.48	2.73	1.96	3.88	4.72	10.68
D_{Fh}	2.61	2.34	1.72	3.42	4.11	10.20
D_{GTh}	2.49	2.36	1.72	3.45	4.13	10.20
$D_{2\nu}$	3.13	3.40	2.06	3.63	4.66	13.64

TABLE VI: Calculated [23, 24] and experimental [56] deformation parameters β_2 of parent and daughter nuclei participating in $(\beta^+\beta^+)_{0\nu}$ and $(\varepsilon\beta^+)_{0\nu}$ modes.

Nuclei	β_2	
	Theory	Experiment
^{96}Ru	0.161	0.1579±0.0031
^{96}Mo	0.191	0.1720±0.0016
^{102}Pd	0.185	0.196±0.006
^{102}Ru	0.232	0.2404±0.0019
^{106}Cd	0.176	0.1732±0.0042
^{106}Pd	0.203	0.229±0.006
^{124}Xe	0.210	0.212±0.007
^{124}Te	0.164	0.1695±0.0009
^{130}Ba	0.234	0.2183±0.0015
^{130}Xe	0.166	0.169±0.007
^{156}Dy	0.300	0.2929±0.0016
^{156}Gd	0.316	0.3378±0.0018

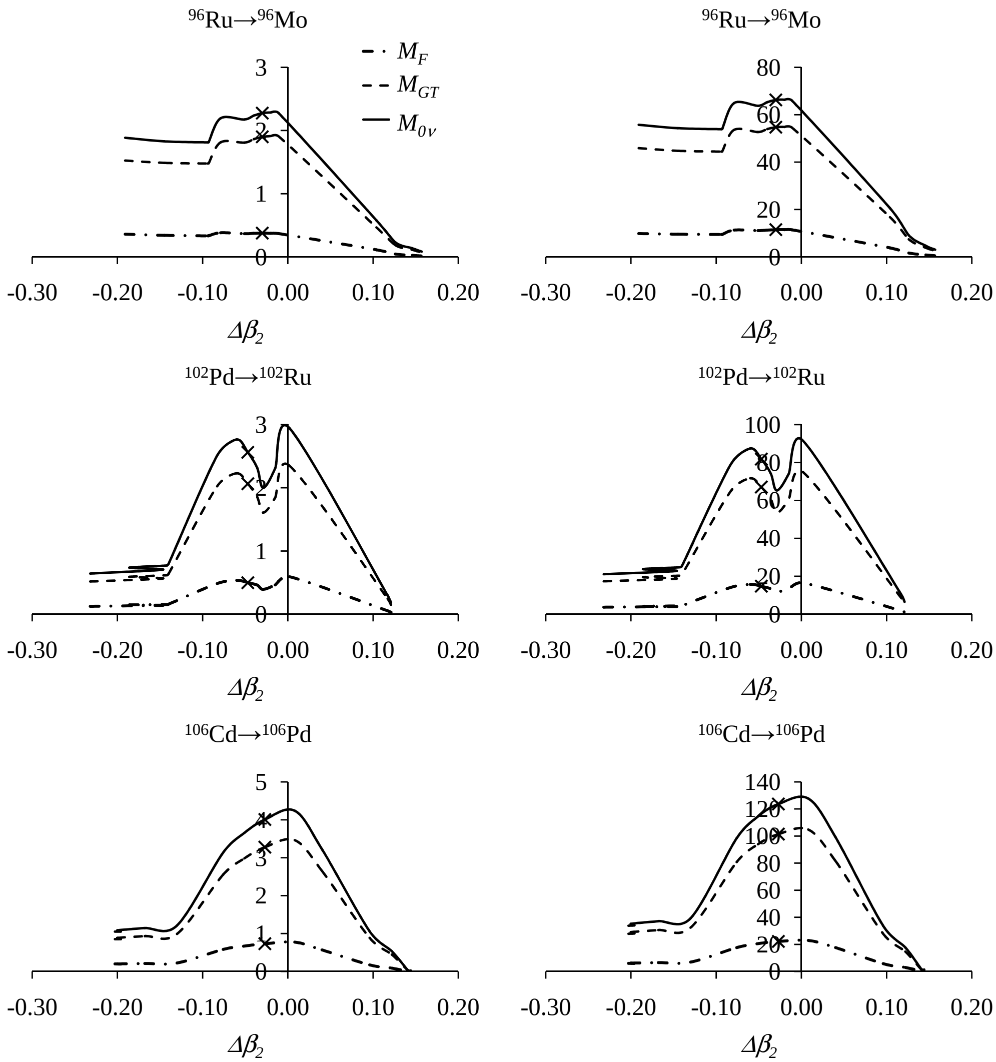

FIG. 2: NTMEs of $(\beta^+\beta^+)_{0\nu}$ and $(\varepsilon\beta^+)_{0\nu}$ modes for ^{96}Ru, ^{102}Pd, ^{106}Cd isotopes due to the exchange of light (left hand side) and heavy (right hand side) neutrinos as a function of the difference in the deformation parameters $\Delta\beta_2$. "×" denotes the NTME for calculated $\Delta\beta_2$ at $\zeta_{qq} = 1$.

IV. CONCLUSIONS

We have calculated the NTMEs M_F, M_{GT}, M_{Fh} and M_{GTh} required to study the $(\beta^+\beta^+)_{0\nu}$ mode of ^{96}Ru, ^{106}Cd, ^{124}Xe and ^{130}Ba as well as the $(\varepsilon\beta^+)_{0\nu}$ mode of ^{96}Ru, ^{102}Pd, ^{106}Cd, ^{124}Xe, ^{130}Ba and ^{156}Dy nuclei for the $0^+ \to 0^+$ transition in the Majorana neutrino mass mechanism using the set of HFB wave functions, the reliability of which was tested by obtaining an overall agreement between theoretically calculated results for the yrast spectra, reduced $B(E2{:}0^+ \to 2^+)$ transition probabilities, static quadrupole moments $Q(2^+)$ and g-factors $g(2^+)$ and NTMEs $M_{2\nu}$ as well as half-lives $T_{1/2}^{2\nu}$ of $(e^+\beta\beta)_{2\nu}$ decay and the available experimental data [23, 24, 34]. The existing experimental data on $(\beta^+\beta^+)_{0\nu}$ and $(\varepsilon\beta^+)_{0\nu}$ modes fail to provide stringent limits on the extracted effective mass of light neutrino $\langle m_\nu\rangle$ and heavy neutrino $\langle M_N\rangle$. Hence, we calculate half-lives $T_{1/2}^{0\nu}$ of these modes for the light neutrino and extract limits on $\langle M_N\rangle$. In the mass mechanism, the half-lives $T_{1/2}^{0\nu}(\beta^+\beta^+)$ and $T_{1/2}^{0\nu}(\varepsilon\beta^+)$ are related through the exactly calculable phase space factors $G_{01}(\beta^+\beta^+)$ and $G_{01}(\varepsilon\beta^+)$. In addition, it is observed that the ratio of NTMEs $|M_{0N}|\,/\,|M_{0\nu}| \approx 30$ is a constant for different nuclei so that half-lives due to the exchange of light and heavy neutrinos are also in constant ratio. Further, the role of deformation on NTMEs M_F, M_{GT}, M_{Fh} and M_{GTh} for $(\beta^+\beta^+)_{0\nu}$ and $(\varepsilon\beta^+)_{0\nu}$ modes is investigated by changing the strength ζ_{qq} of the QQ interaction. It is noticed that there is an inverse correlation between the magnitudes of NTMEs and quadrupole moments $Q(2^+)$ as well as deformation parameters β_2. The NTMEs are suppressed by factors of 1.7–10.7 in the considered mass range $A = 96 - 156$ implying that the nuclear struc-

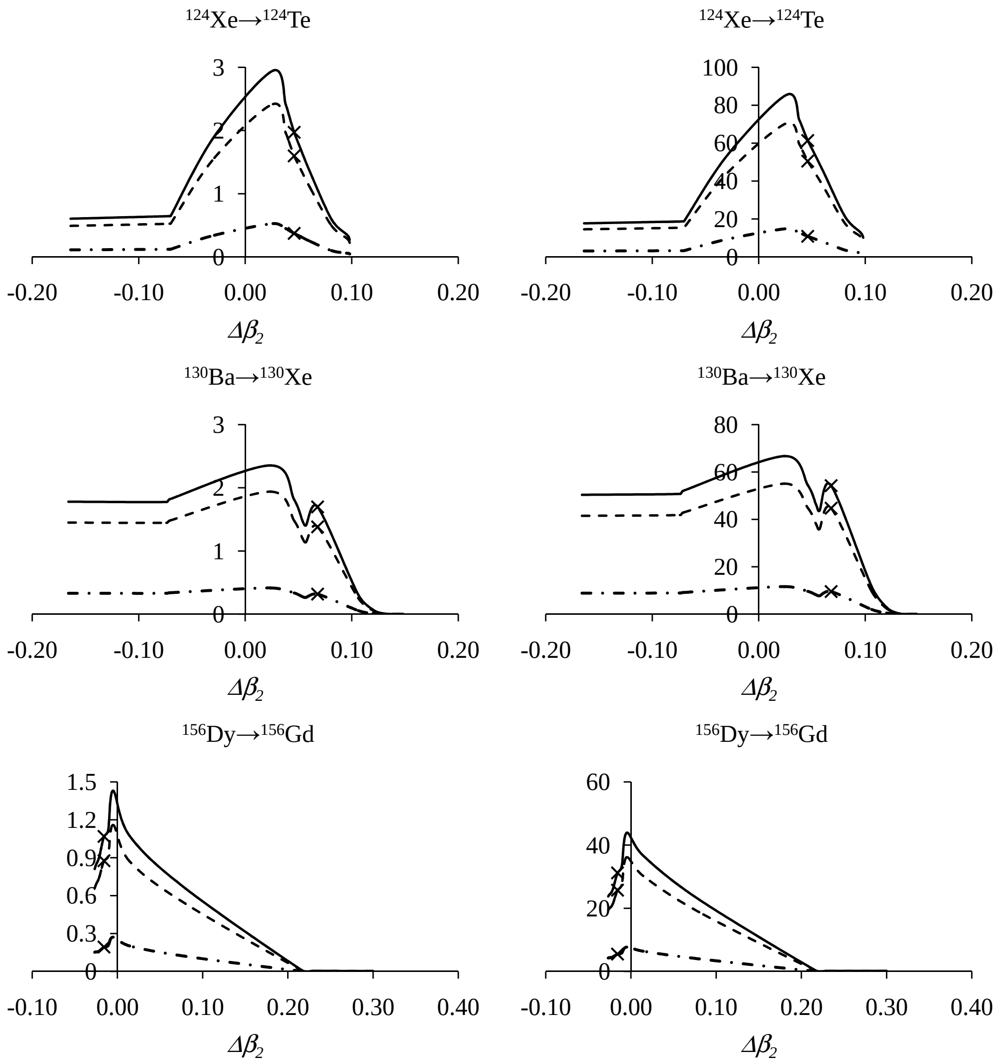

FIG. 3: NTMEs of $\left(\beta^{+}\beta^{+}\right)_{0\nu}$ and $\left(\varepsilon\beta^{+}\right)_{0\nu}$ modes for ^{124}Xe,^{130}Ba and ^{156}Dy isotopes. Further details are given in Fig. 2.

ture effects are also important for $(\beta^{+}\beta^{+})_{0\nu}$ and $(\varepsilon\beta^{+})_{0\nu}$ modes. The deformation of individual nucleus is an important parameter for calculating NTMEs $M_{0\nu}$ and M_{0N} of $(\beta^{+}\beta^{+})_{0\nu}$ and $(\varepsilon\beta^{+})_{0\nu}$ modes.

This work has been partially supported by DST, India vide grant No. SR/S2/HEP-13/2006, by Conacyt-México and DGAPA-UNAM.

[1] F. T. Avignone III, S. R. Elliott, J. Engel, Rev. Mod. Phys. **80**, 481 (2008).
[2] S. P. Rosen and H .Primakoff, in *Alpha-beta-gamma ray spectroscopy*, edited by K. Siegbahn (North-Holland, Amsterdam, 1965), Vol. II, p. 1499
[3] J. D. Vergados, Nucl. Phys. **B218**, 109 (1983).
[4] J. D. Vergados, Phys. Rep. **133**, 1 (1986).
[5] M. Doi and T. Kotani, Prog. Theor. Phys. **87**, 1207 (1992).
[6] M. Doi and T. Kotani, Prog. Theor. Phys. **89**, 139 (1993).
[7] A. S. Barabash, in *Proceedings of International Workshop on Double Beta Decay and Related Topics*, edited by H. V. Klapdor and S. Stoica (World Scientific, Singapore, 1996).
[8] J. Suhonen and O. Civitarese, Phys. Rep. **300**, 123 (1998).
[9] I. V. Kirpichnikov, Phys. At. Nucl. **63**, 1341 (2000).
[10] H. V. Klapdor-Kleingrothaus, *Sixty years of Double Beta Decay,* World Scientific, Singapore (2001).
[11] A. S. Barabash, Phys. At. Nucl. **67**, 438 (2004).
[12] P. Bamert, C. P. Burgess and R. N. Mohapatra, Nucl. Phys. **B449**, 25 (1995).
[13] M. Hirsch, K. Muto, T. Oda, and H. V. Klapdor- Kleingrothaus, Z. Phys. A **347**, 151 (1994).

[14] H. V. Klapdor-Kleingrothaus, I. V. Krivosheina, A. Dietz, and O. Chkvorets, Phys. Lett. **B586**, 198 (2004).
[15] H. V. Klapdor-Kleingrothaus, I. V. Krivosheina, and I. V. Titkova, Int. J. Mod. Phys. A **21**, 1159 (2006).
[16] Z. Sujkowski and S. Wycech, Phys. Rev. C **70**, 052501(R) (2004).
[17] A. S. Barabash, Ph. Hubert, A. Nachab, S. I. Konovalov, I. A. Vanyushin, and V. Umatov, Nucl. Phys. **A807**, 269 (2008).
[18] A. Griffiths and P. Vogel, Phys. Rev. C **46**, 181 (1992).
[19] J. Suhonen and O. Civitarese, Phys. Rev. C **49**, 3055 (1994).
[20] E. Caurier, J. Menéndez, F. Nowacki, and A. Poves, Phys. Rev. Lett. **100**, 052503 (2008).
[21] J. Menéndez, A. Poves, E. Caurier, and F. Nowacki, arXiv:0809.2183v1[nucl-th].
[22] R. Chandra, J. Singh, P. K. Rath, P. K. Raina, and J. G. Hirsch, Eur. Phys. J. A **23**, 223 (2005).
[23] P. K. Raina, A. Shukla, S. Singh, P. K. Rath, and J. G. Hirsch, Eur. Phys. J. A **28**, 27 (2006); A. Shukla, P. K. Raina, R. Chandra, P. K. Rath, and J. G. Hirsch, Eur. Phys. J. A **23**, 235 (2005).
[24] S. Singh, R. Chandra, P. K. Rath, P. K. Raina, and J. G. Hirsch, Eur. Phys. J. A **33**, 375 (2007).
[25] K. Chaturvedi, R. Chandra, P. K. Rath, P. K. Raina, and J. G. Hirsch, Phys. Rev. C. **78**, 054302 (2008).
[26] R. Chandra, K. Chaturvedi, P. K. Rath, P. K. Raina, and J. G. Hirsch, Europhys. Lett. **86**, 32001 (2009).
[27] P. Vogel and M. R. Zirnbauer, Phys. Rev. Lett. **57**, 3148 (1986).
[28] O. Civitarese, A. Faessler, and T. Tomoda, Phys. Lett. **B194**, 11 (1987).
[29] F. Šimkovic, L. Pacearescu, and A. Faessler, Nucl. Phys. **A733**, 321 (2004); L. Pacearescu, A. Faessler, and F. Šimkovic, Phys. At. Nucl. **67**, 1210 (2004).
[30] M. S. Yousef, V. Rodin, A. Faessler, and F. Šimkovic, Phys. Rev. C **79**, 014314 (2009).
[31] R. Álvarez-Rodríguez, P. Sarriguren, E. Moya de Guerra, L. Pacearescu, A. Faessler, and F. Šimkovic, Phys. Rev. C **70**, 064309 (2004).
[32] V. Rodin and A. Faessler, Phys. Rev. C **77**, 025502 (2008).
[33] M. Baranger and K. Kumar, Nucl. Phys. **A110**, 490 (1968).
[34] P. K. Rath, R. Chandra, S. Singh, P. K. Raina, and J. G. Hirsch, arXiv:0906.4014v1[nucl-th].
[35] F. Šimkovic, G. Pantis, J. D. Vergados, and A. Faessler, Phys. Rev. C **60**, 055502 (1999).
[36] J. D. Vergados, Phys. Rep. **361**, 1 (2002).
[37] J. G. Hirsch, O. Castaños, and P. O. Hess, Nucl. Phys. **A582**, 124 (1995).
[38] M. Kortelainen and J. Suhonen, Phys. Rev. C **76**, 024315 (2007); M. Kortelainen, O. Civitarese, J. Suhonen, and J. Toivanen, Phys. Lett. **B647**, 128 (2007).
[39] F. Šimkovic, A. Faessler, V. Rodin, P. Vogel, and J. Engel, Phys. Rev. C **77**, 045503 (2008).
[40] F. Šimkovic, A. Faessler, H. Muether, V. Rodin, and M. Stauf, Phys. Rev. C **79**, 055501 (2009).
[41] G. A. Miller and J. E. Spencer, Ann. Phys. **100**, 562 (1976).
[42] H. F. Wu, H. Q. Song, T. T. S. Kuo, W. K. Cheng, and D. Strottman, Phys. Lett. **B162**, 227 (1985).
[43] N. Onishi and S. Yoshida, Nucl. Phys. **80**, 367 (1966).
[44] G. M. Heestand, R. R. Borchers, B. Herskind, L. Grodzins, R. Kalish, and D. E. Murnick, Nucl. Phys. **A133**, 310 (1969).
[45] W. Greiner, Nucl. Phys. **80**, 417 (1966).
[46] W. C. Haxton and G. J. Stephenson, Jr., Prog. Part. Nucl. Phys. **12**, 409 (1984).
[47] J. Menéndez, A. Poves, E. Caurier, and F. Nowacki, Nucl. Phys. **A818**, 139 (2009).
[48] Eric B. Norman, Phys. Rev. C **31**, 1937 (1985).
[49] F. A. Danevich, A. Sh. Georgadze, V. V. Kobychev, B. N. Kropivyansky, A. S. Nikolaiko, O. A. Ponkratenko, V. I. Tretyak, S. Yu. Zdesenko, Yu. G. Zdesenko, P. G. Bizzeti, T. F. Fazzini, and P. R. Maurenzig, Phys. Rev. C **68**, 035501 (2003).
[50] A. S. Barabash, V. V. Kuzminov, V. M. Lobashev, V. M. Novikov, B. M. Ovchinnikov, and A. A. Pomansky, Phys. Lett. **B223**, 273 (1989).
[51] A. S. Barabash and R. R. Saakyan, Phys. At. Nucl. **59**, 179 (1996).
[52] A. Staudt, K. Muto, and H. V. Klapdor-Kleingrothaus, Phys. Lett. **B268**, 312 (1991).
[53] S. Stoica and H. V. Klapdor-Kleingrothaus, Eur. Phys. J. A **17**, 529 (2003).
[54] J. Suhonen and M. Aunola, Nucl. Phys. **A723**, 271 (2003).
[55] M. Aunola and J. Suhonen, Nucl. Phys. **A643**, 207 (1998).
[56] S. Raman, C. W. Nestor Jr. and P. Tikkanen, Atomic data and Nuclear data Tables **78**, 1 (2001).